

# A 16-channel avalanche photodiode detector array for visible and near-infrared flow cytometry

William G. Lawrence<sup>a</sup>, Christopher Stapels<sup>a</sup>, Richard Farrell<sup>a</sup>, Joseph D. Tario, Jr.<sup>b</sup>, Edward Podniesinski<sup>b</sup>, and Paul K. Wallace<sup>b</sup>, James F. Christian<sup>a</sup>

<sup>a</sup>Radiation Monitoring Devices, 44 Hunt St., Watertown MA 02472;

<sup>b</sup>Roswell Park Cancer Institute, Elm and Carlton Streets, Buffalo NY 14263

## ABSTRACT

We report on the development and application of a flow cytometer using a 16-channel avalanche photodiode (APD) linear detector array. The array is configured with a dispersive grating to simultaneously record emission over a broad wavelength range using the 16 APD channels of the linear APD array. The APD detector elements have a peak quantum efficiency of 80% near 900 nm and have at least 40% quantum efficiency over the 400-nm to 1000-nm wavelength range. The extended red sensitivity of the detector array facilitates the use of lower energy excitation sources and near IR emitting dyes which reduces the impact of autofluorescence in signal starved measurements. The wide wavelength sensitivity of the APD array permits the use of multiple excitation sources and many different fluorescent labels to maximize the number of independent parameters in a given experiment. We show the sensitivity and linearity measurements for a single APD detector. Initial results for the flow cytometer with the 16-element APD array and the 16-channel readout ASIC (application specific integrated circuit) are presented.

Keywords: Flow cytometry, APD, Avalanche Photodiode, detector array, NIR, near infrared

## 1. INTRODUCTION

Multicolor analysis in flow cytometry is an important tool to phenotype cells, analyze immune system responses and characterize dynamics of cell growth and apoptosis. The multicolor cytometer systems provide greater specificity in cell identification and enable detailed studies of small sample volumes. The use of sensitive detectors with improved near infrared response and the development of new infrared emitting dyes [1, 2] and quantum dots[3, 4] will extend the working wavelength range of the multicolor flow cytometer systems. Avalanche photodiodes (APDs) are solid-state silicon photodetectors that have high detection efficiency in visible wavelength region and into the near infrared. These devices detect light from below 300 nm to 1100 nm with a quantum efficiency (Q.E.) greater than 50% from 400 nm to 1000 nm. Like the traditional photomultiplier detector, avalanche photodiodes multiply the initial photo-generated signal. Avalanche photodiodes, however, can be much smaller than existing photomultiplier tubes. The smaller size and improved quantum efficiency of the APDs can be used to create smaller flow cytometers with an improved range of spectral response.

From the initial development of three parameter flow cytometry that used side scatter, forward scatter, fluorescence [5], there has been an effort to increase the number of parameters that an instrument can monitor to improve the differentiation of cells [6]. This has been accomplished by increasing the number of excitation sources and detectors to measure different fluorescent wavelengths. New laser sources from the near ultraviolet to the near infrared have been used to excite different fluorescent labels. Tandem dyes using fluorescent resonant energy transfer have been developed to shift the emission wavelength and efficiently use the available spectral range. Efforts to extend the usable spectral range into the near infrared have been limited by the poor detection efficiency of PMTs in that region. Recent reports on the modification of available instruments [2] and new designs of commercial instruments have shown that avalanche photodiodes can be used for flow cytometry studies in the near IR spectral region.

Avalanche photodiodes operate at high reverse bias to multiply the initial photogenerated charge carriers. The avalanche mechanism occurs when the electric field is sufficiently strong that existing charge carriers create new

charge carriers by impact ionization. RMD manufactures silicon APDs with active areas from 0.5mm<sup>2</sup> to 4000 mm<sup>2</sup>. These devices have gains over 10,000 at room temperature, and over 40,000 when cooled to -30°C [7]. These devices have fast temporal response and high quantum efficiency across the visible and near infrared spectrum. The peak of the quantum efficiency is 80% at 900 nm [8]. In this report, we focus on the development of a multicolor flow cytometry system that uses a compact concave grating for wavelength dispersion and a 16-element APD array for fluorescence detection. The detector array is a 1 x 16 linear arrangement of 2mm x 2mm APD elements. The total length of the array is 4 cm and currently covers a spectral range from 540 nm to 660 nm in 16 channels. We have also developed a multi-channel miniaturized preamplifier readout ASIC (application specific integrated circuit) to simplify the data acquisition.

## 2. EXPERIMENTAL SYSTEMS

### 2.1 RPCI Instrument

Two different flow cytometer test systems are used to examine the performance of the APD detectors. The Roswell Park Cancer Institute maintains a state-of-the-art flow cytometry facility that operates many flow cytometers as a shared facility. One of the commercial instruments, the LSR-1 (Becton Dickinson Biosciences (BDB), San Jose CA), has been modified to accept a 785-nm laser and an APD detector. The details of the modifications and the system layout have been described previously[2]. The most relevant of the modifications was the addition of 785-nm source at the third laser position, and the addition of the APD detector at the P8 (FL6) position. Radiation Monitoring Devices supplied the APD detector. The APD was mounted in a cylinder of Delrin and inserted into the PMT holder. The performance of the system was calibrated with 5.1 μm IR-sensitive beads from Spherotech (Libertyville IL).

### 2.2 RMD Instrument

The RMD flow cytometer is a brass-board instrument designed primarily from off-the-shelf components. This design prototype demonstrates the detection of the cytometer fluorescence with the APD array and provides a platform to evaluate other detectors. Figure 1 shows the major components of the RMD flow cytometer and illustrates the position of the single element APD detector and the APD array. The excitation source is a Cyonics model 2201 laser at 488 nm that is operated with an output of 4 – 9 mW. A prism block (PB) is used to shape the laser beam output and a turning mirror assembly (M1) is used for beam steering. A focusing lens (L1) is used to control the beam shape in the flow cell. The fluorescence signal is collected by lens (L2) to form an image in the plane of the iris. The iris spatially separates fluorescence and scatter signal from the sample flow volume from scattered laser light at the edges of the capillary. A dichroic 540-nm long-pass beam splitter separates the scattered light from the fluorescent light. The side scatter is directed to a PMT, while the fluorescence passes through the filter. The fluorescence can be detected using either a single element APD or the APD array. A removable single element platform can be placed behind the dichroic filter. The platform consists of a collection lens, a band pass filter (BP2) and a single element APD detector. We used a 585-nm filter with a 42-nm band pass for the fluorescence channel.

The signal from the single element APD detector was processed using a Canberra model 2004 preamplifier and a Canberra model 2025 Research Amplifier. The amplifier output was recorded using an Oxford Instruments multichannel analyzer (MCA) and stored on a personal computer. The side scatter signal from the PMT is used to gate the MCA. If the single element platform is removed, the fluorescence is directed to a concave holographic grating (Richardson Grating Laboratory) that produces a spectrally resolved line image at the focal plane of the concave grating. The sixteen element APD array sits at the focus of the grating. The array is mounted on a board that includes the high voltage control electronics and the data acquisition ASIC.

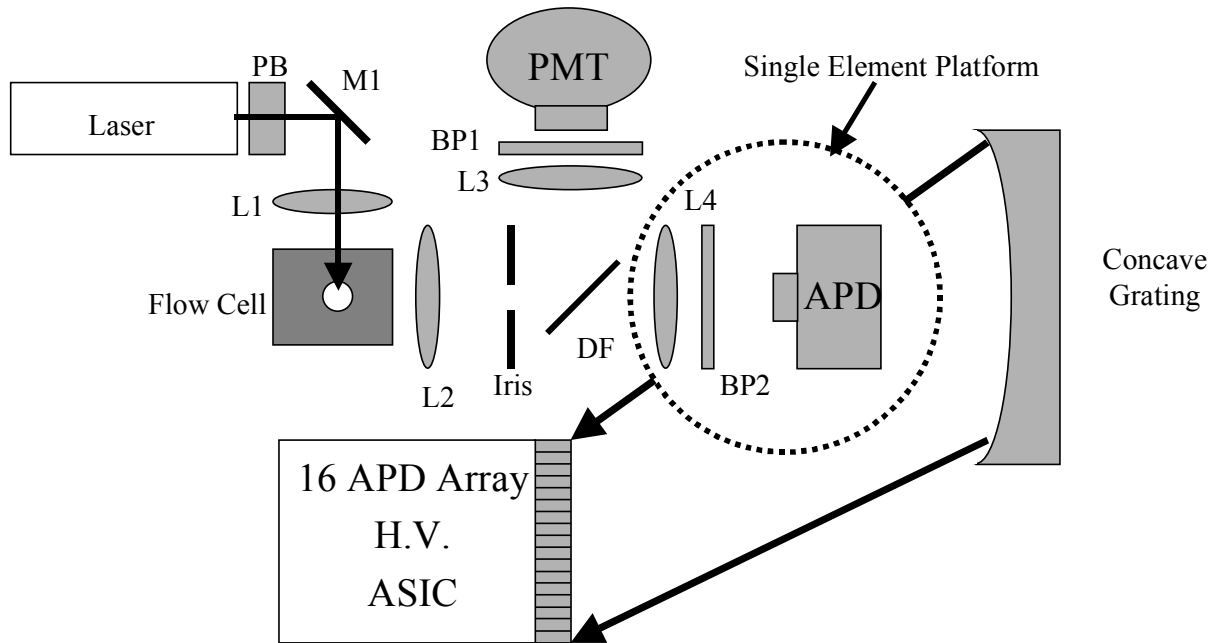


Figure 1: Schematic illustration of the RMD flow cytometer. This figure illustrates the detection optics, the concave grating, and the placement of the 16 element APD array. The Single Element Platform within the circle is removed for multi-channel operation. The details of the figure are described in the text.

### 2.3 ASIC for 16-element APD array

A proprietary ASIC (RMD and Augustine Engineering, Encinitas CA) has been developed for the front end of the detector interface to handle the asynchronous data collection from the 16 element APD array. Figure 2 shows the block diagram for the operation of the ASIC and illustrates the functional components of the system. Many of the functional elements of the ASIC have user defined settings that are programmed by an external interface. These settings include the preamp gain factor, the shaping coefficients, and peak hold widths. The ASIC contains 16 input channels that are represented by the components above the dotted line in Figure 2. The output of each APD detector is connected to the input of one of the ASIC channels. The charge pulse from the APD is converted to a voltage at the preamplifier stage. The preamplifier gain is selected by the user and ranges from  $1 \times 10^{-6}$  Volts per electron to  $5 \times 10^{-6}$  volts per electron. After the polarity selection each of the signals is relayed to a fast and slow shaper circuit. Both shaper outputs can be read out directly, and it can also be used to set a trigger. Any of the 16 local trigger outputs can be used to initiate the data acquisition. The trigger can also come from an external source as illustrated in Figure 2. When the system is triggered, the output of the slow shaper is acquired by a peak hold circuit. The output of the peak hold circuit is available at the slow analog output for each trigger event. This signal is a square pulse and the amplitude of the pulse is proportional to the APD input. The temporal width of the pulse is long enough to sample all 16 of the output channels with a conventional analog-to-digital circuit. The ASIC is designed to output the intensity of all 16 APD channels whenever one of the APD channels is triggered. Alternatively, the ASIC can output the intensity of all 16 APD channels when it receives an external trigger from the forward or side scatter detector output.

### 2.4 Absolute intensity calibration

In the course of the experiments at RMD we have been able to perform absolute intensity calibrations of the APD detector in terms of the incident photon intensity. This allows us to determine the number of photons incident on the detector for each fluorescence event in the flow cell. The absolute calibration of the APD response is measured using a radioactive  $^{55}\text{Fe}$  source. The radioactive decay of the  $^{55}\text{Fe}$  produces an x-ray photon at 5.9 keV. The absorption of the photon produces a localized pulse of 1600 electron / hole pairs. These electron-hole pairs create additional charge carriers by impact ionization. The efficiency of the charge multiplication is determined by the

operating bias of the APD detectors. This APD output is related to the output expected for each incident photon. The quantum efficiency (Q.E.) defines the probability that a photon will create an electron-hole pair for amplification in the APD. The quantum efficiency is wavelength dependent, but is typically about 0.6. It requires  $1639/(Q.E.)$  photons (or about 2730) visible or near IR photons to produce the same output signal as a single  $^{55}\text{Fe}$  x-ray photon event. This relationship establishes an absolute calibration of the APD response.

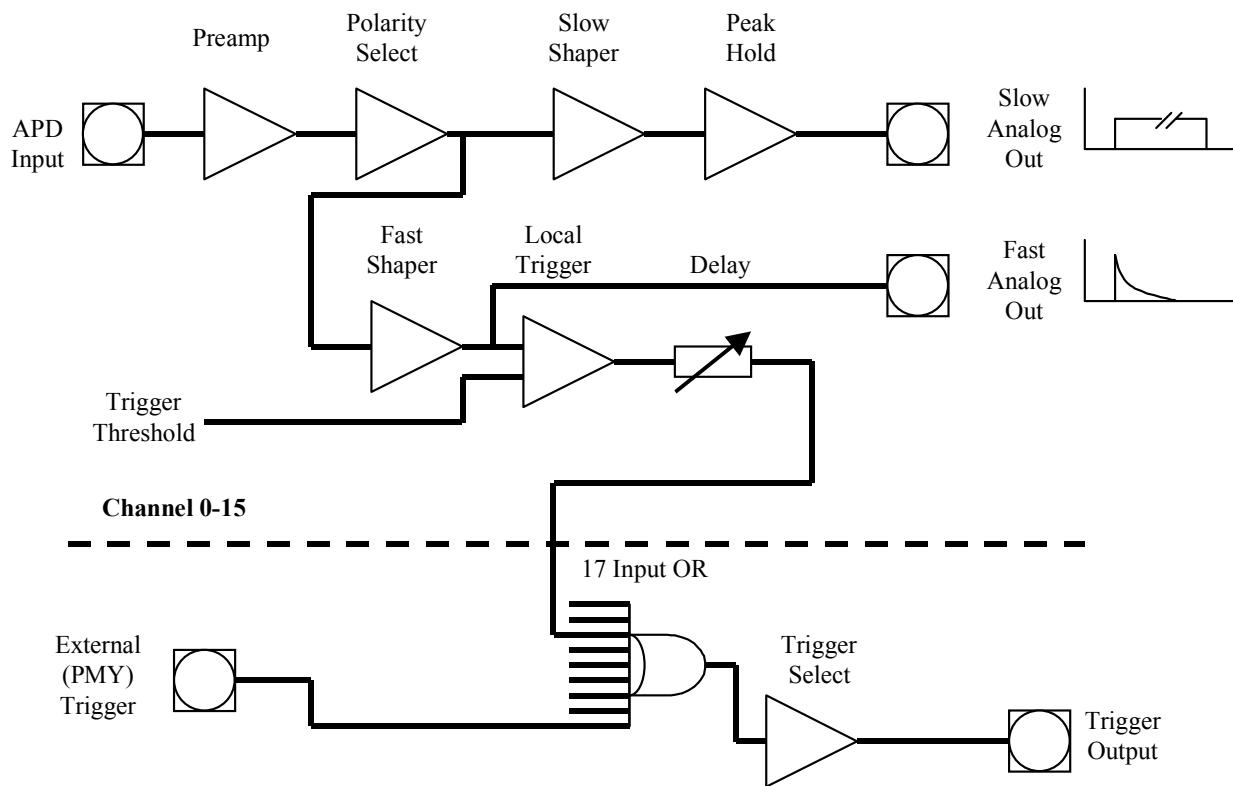


Figure 2: Block diagram of the operation of the ASIC (Application Specific Integrated Circuit) that is used for the 16 element APD array readout. The 16 input channels are represented by the circuit shown above the dashed line, and the gate circuit, which is common to the array, is shown below the dashed line.

### 3. SINGLE ELEMENT APD RESULTS

#### 3.1 Single element APD calibration

We have made some initial measurements on the RMD prototype flow cytometer to demonstrate the performance of the instrument with a single APD detector element. These studies are intended to compare the performance of the APD based system to a PMT based system and to quantify the anticipated signal levels. Figure 1 shows the experimental setup using a single detector element. We have measured the fluorescence of  $6.3\ \mu\text{m}$  Sphero Rainbow calibration beads (Spherotech). This sample contains similar sized particles with six different fluorescence intensities. The fluorescence intensities are calibrated by the manufacturer in terms of milli FITC equivalents (MEFL). In this study we have used a bandpass filter centered at 530 nm with a 30 nm bandpass that reproduces the FL1 spectral region. The APD is biased with a voltage of 1780 V, and the output signal is amplified using the Canberra preamp and amplifier. The amplifier output was recorded using a 2048 multichannel analyzer that was gated by the side scatter signal from the PMT shown in Figure 1.

Figure 3a shows the APD channel histogram for the Spherotech 6-peak bead set measured with a 488-nm laser excitation power of 9 mW. The APD output has been calibrated in terms of the incident photon intensity using the

iron-55 calibration procedure described earlier. The dynamic range of the measurement is limited by the 2048 (11 bit) resolution of the MCA. The MCA records the signal from the linear spectroscopy amplifier and Figure 3a plots this data on a log scale. The plot shows the 6 peaks that are expected in the calibration set. The peak position provides a measure of the photon flux at the detector for the dye loading of the different beads. Figure 3b shows the linear relationship between the dye loading of the beads that was measured by the manufacturer and the photon intensity that is measured at the APD detector. The fluorescence emitted by the beads depends on the laser pump power and beam focussing conditions. The number of photons that reach the detector depends on the geometry of the collection optics and the details of the filters used to isolate the signal. In this case, we detect about 0.75 photons per milli-equivalent fluorescence (MEFL) from the beads with an input laser power of 9 mW.

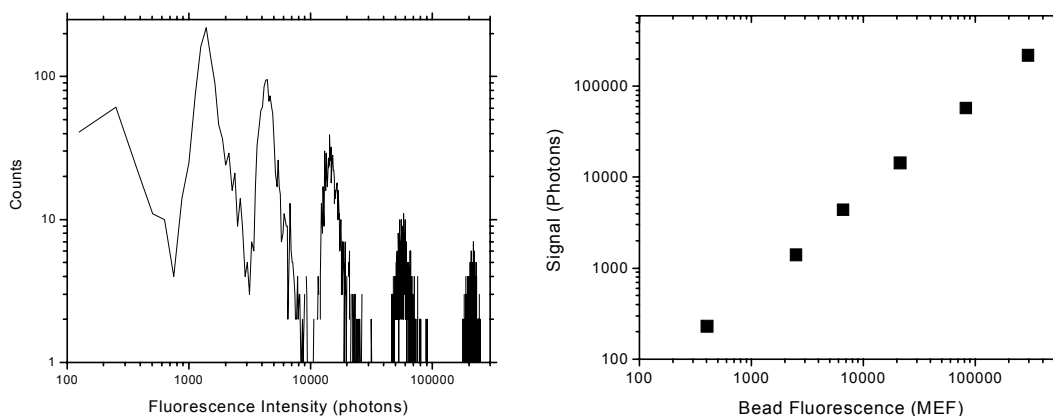


Figure 3: a) Histogram for the detection of the Spherotech 6-peak bead set recorded using the single APD detector element. b) Plot of the photon intensity that is detected by the APD as a function of the calibrated bead fluorescence intensity that was provided by the manufacturer (Spherotech).

### 3.2 Near IR proliferation studies

To further evaluate the utility of the single element APD detector in the near infrared, we used a prototype tracking dye developed by PTI Research (Malvern, PA) on the RPCI instrument [2] to measure proliferation. This dye is structurally related to the PKH class of lipophilic tracking dyes used to homogeneously label and track cells [9]. These dyes are retained in the cell membrane and do not adversely affect cellular function. They can be used to monitor cell proliferation, because during each round of cell division the relative intensity of the dye per cell decrease by half as it becomes equally distributed between the daughter cells.

Using these dyes to analyze cell proliferation provides several distinct advantages over traditional methods. First, the use of  $^3\text{H}$  thymidine for proliferation studies does not allow for positive identification or quantification of the proliferating cell population and requires the handling of radioactive materials. Analysis of antigen-specific T cell proliferation is a novel and informative application of this technique [10]. Lymphocytes are first labeled with the dye and then cultured for 4 - 8 days with the antigen of interest. At culture termination, the cells are harvested and identified using fluorescently labeled antibodies to cell surface molecules. This permits enumeration and detailed characterization of the specific lymphocyte subsets responding to the antigen.

The current generation of PKH dyes are excited at or near 488 nm and are detected either in the FL1 (530/30 nm) or FL2 (585/42 nm) channels which are normally reserved for FITC or PE, respectively. Using these channels to detect the tracking dyes limits the number of antibodies which may be used to characterize the proliferating cells. Moreover, there are spectral overlap issues which can further limit their usefulness on conventional flow cytometers. To increase the number of channels available to characterize proliferating cells, PTI Research has developed the CellVue NIR tracking dye. This dye is structurally similar and used in the same way to track cell proliferation as

PKH26 (Sigma, St. Louis, MO, [9]). It is excited at 785 nm and emits optimally at 834 nm. At this detection wavelength, a standard PMT has very poor efficiency, whereas it is near optimal for an APD.

We evaluated the feasibility of using the NIR tracking dye and the near infrared to track cell proliferation on the RPCI APD flow cytometer with the APD detector. The U937 cell line was labeled with CellVue NIR as previously described for PKH26 [11]. Briefly, U937 cells were washed and resuspended in Diluent C at twice the final staining concentration and then immediately combined with an equal volume of CellVue NIR in Diluent C. Final staining conditions were  $5 \times 10^6$  cells/ml in 10  $\mu$ M CellVue NIR. After 3 minutes at room temperature, the staining reaction was stopped with an equal volume of FCS. Stained cells were pelleted, transferred to a fresh centrifuge tube and washed twice with complete medium (CM, RPMI 1640, supplemented with 10% heat-inactivated FCS; 0.1 mM non-essential amino acids, 0.1 mM sodium pyruvate and 50  $\mu$ g/ml gentamicin, 2 mM fresh glutamine, Invitrogen, Carlsbad, CA; and  $5 \times 10^{-5}$  M 2-mercaptoethanol, Sigma-Aldrich Corporation., St. Louis, MO). The cells were then placed into culture at  $2.5 \times 10^5$  cells/ml and incubated at 37°C for 5 days. Samples were taken daily and analyzed on the RPCI Instrument.

The results from Day 1 and 4 of culture are shown in Figure 4. On Day 1, the MFI was 1696 and the histogram had a symmetrical shape indicative of homogeneous staining which is critical for accurately following proliferation. The cell count was  $4.9 \times 10^5$  cells/ml. By Day 4, the MFI had dropped to 223 while the cell number had increased to  $3.6 \times 10^6$  cells/ml. During culture, the fluorescence intensity of the U937s had decreased 7.6 fold while the cell number had increased a corresponding 7.3 fold. The correlation between the decrease in fluorescence and increase in cell number indicates that the (i) APD's sensitivity and linearity is suitable for tracking proliferation (ii) and that the CellVue NIR dyes should be further developed.

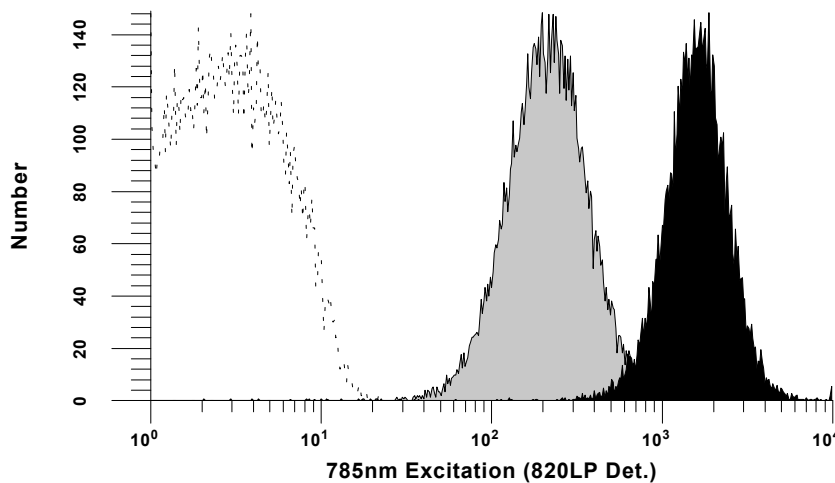


Figure 4: Proliferation of U937 cells stained with the CellVue NIR tracking dye revealing the dye dilution of the cells as they divide in culture. U937 cells were stained and then placed into culture. Samples were collected on Day 1 (black filled histogram), and on Day 4 (gray filled histogram); Unstained cells (dotted line) are included for reference.

## 4. SIXTEEN ELEMENT APD ARRAY RESULTS

### 4.1 APD array wavelength calibration

The design of this multi-channel flow cytometer is based on the separation of the fluorescence signal by a concave grating. Figure 1 illustrates the grating and detector geometry for the multi-channel instrument (Note: The single element detector platform within the circle is removed for multi-channel operation.) The concave grating provides spectral separation of the fluorescence from the flow cell and focuses the spectrally resolved emission into a line at

the detector array. Each detector element will be illuminated by a narrow band of emission wavelengths. The position of the detector array defines the wavelength band that will hit each APD element.

The spectral sensitivity of each APD element was calibrated by scanning the output of a monochromator with a 4 nm bandpass. The spectrally resolved light was generated using the emission from a white LED through a short-path Optometrics monochromator. The white LED was driven by a pulser to provide a 5 microsecond light pulse that was compatible with the time constant of the detection electronics and was similar to the flow emission. The monochromator output passed through an optical fiber and was emitted at the iris image plane shown in Figure 1. The light output illuminated the grating which focussed the light onto the different detector elements. As the monochromator wavelength was adjusted, different APD elements would respond. Figure 5 shows the wavelength band to which each detector responded.

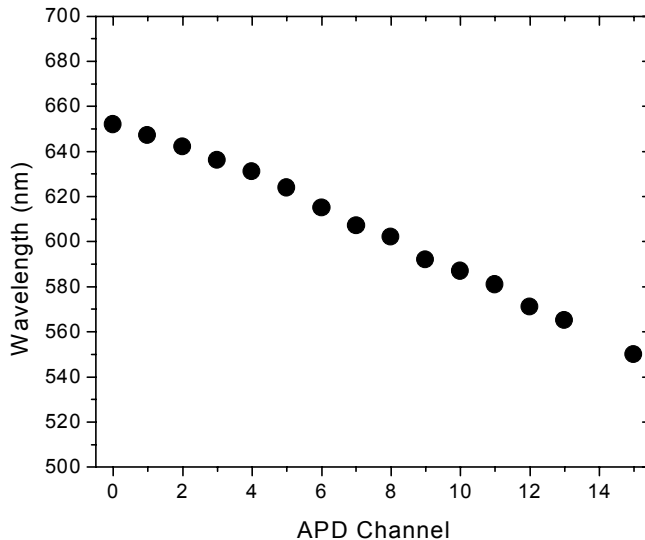


Figure 5: Center wavelength of the response for each of the APD detectors in the array. (Channel 14 is not connected)

The spectral bandpass of each detector is approximately 20 nm, and there is significant overlap between the spectral bands. The limits on the spectral range are controlled by the placement of the APD array. In this case the APD is positioned such that the last APD detects the 540 nm emission. The emission intensity falls off rapidly below 540 nm due to the 540 nm dichroic mirror in the beam path. Some of the spectral overlap is controlled by the placement of the grating and detector array, and also the 4-nm bandpass of the monochromator. The size and placement of the grating constrained the placement of the optical elements in the prototype instrument layout. The position of the grating is not optimized for spectral resolution, but does provide an acceptable focus at the detector plane. The detector channels are labeled as 0 – 15. Channel 14 had a high noise level and was disconnected from the readout interface.

## 4.2 16 Channel APD array flow measurements

We have measured the fluorescence signals from Align Flow Plus beads (Invitrogen Carlsbad California) using the 16 element APD array. Each channel was recorded sequentially using the APD array and the fast analog output of the ASIC. The fast analog output of the ASIC was connected to the Canberra amplifier, and the amplifier output was recorded by the MCA. The channel number of the MCA corresponds to the fluorescence signal measured at the APD. The fluorescence intensity at the APD was calibrated using the iron-55 x-ray emitter source. Figure 6 shows the histogram measured at each APD channel. The wavelength range for each pixel was determined in the previous section. The 488 nm side scatter was used as the trigger source in these measurements.

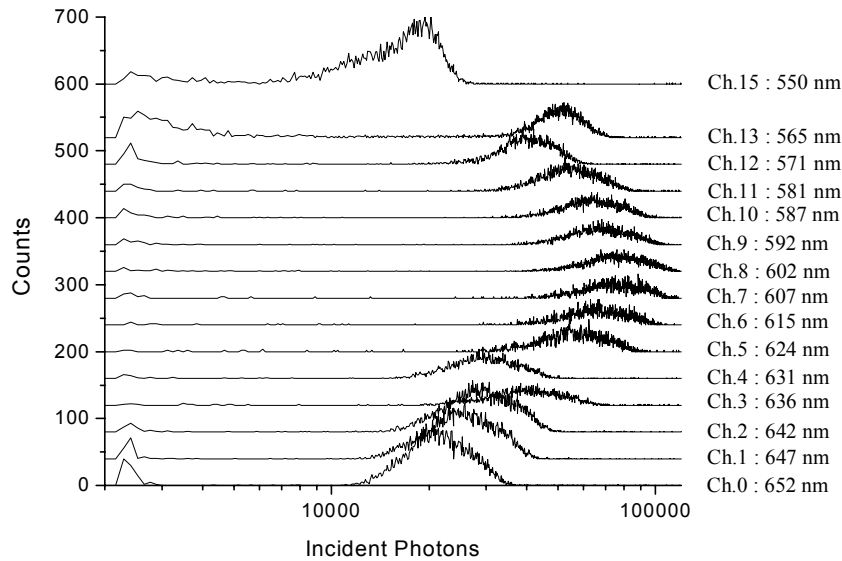


Figure 6: Fluorescence signals from the Align Flow Plus flow cytometry beads recorded for each of the APD array channels. (Channel 14 was not recorded)

#### 4.2 16 Channel APD array measurements with the readout ASIC

A 16-channel preamp ASIC has been developed to simplify the APD readout and minimize the size and power requirements of the electronic processing. A block diagram of the functional components of the ASIC is shown in Figure 2. Each APD detector element is connected to one channel of the ASIC readout circuit. When the ASIC is triggered the maximum of the peak voltage from the APD is held at the analog output of the ASIC. The trigger source can be any or all of the APD detector channels, and can also be provided as an external input. The APD signal is available at the analog output for a user-defined interval. During this interval an analog to digital interface is used to record the APD output and save all 16 channel signals on a personal computer. We have written a program that uses a Kiethley I/O card to read and display the real-time data.

We have recorded the emission spectrum of a pulsed white light emitting diode (LED) to demonstrate the sensitivity and noise in the readout ASIC. A white LED is placed on the sample side of the iris image plane shown in Figure 1. The positions of the grating and APD array are also shown in Figure 1. The LED is driven by a pulsed voltage source with a 2  $\mu$ sec pulse width to simulate the fluorescent light from a labeled particle in the interrogation region of the sample cell. The trigger signal for the ASIC was provided by the PMT. The PMT was illuminated by the LED output that was reflected by the 540 nm beamsplitter. The signal amplification was done within the readout ASIC. The signals from all of the APDs in the array are recorded for each trigger event by a 16 channel analog to digital data collection card (Kiethley) in a personal computer. The data collection card digitizes the output of the sample and hold circuit in each channel of the readout ASIC. A software program has been written to operate the Kiethley data acquisition card in an asynchronous mode. The program handles the data acquisition and storage.

Figure 7a shows the histograms recorded simultaneously from each of the APD channels with the white LED illumination. Note that channel 14 was disconnected from the APD array. The MCA channel number or output voltage is proportional to the intensity of light within the band pass of each APD. The width of the peaks is an indication of the noise associated with the measurement. Figure 7b shows the intensity of the emission at the center of each spectral band pass. The spectrum is not corrected for the wavelength dependent sensitivity of the APD detector or for the throughput of the grating and filters. The emission intensity falls near 540 which is the

transmission edge of the beam splitter. We would also expect the intensity of the LED to fall off at longer wavelengths. These spectra demonstrate that all of the APD signals can be recorded simultaneously with the trigger signal from the PMT.

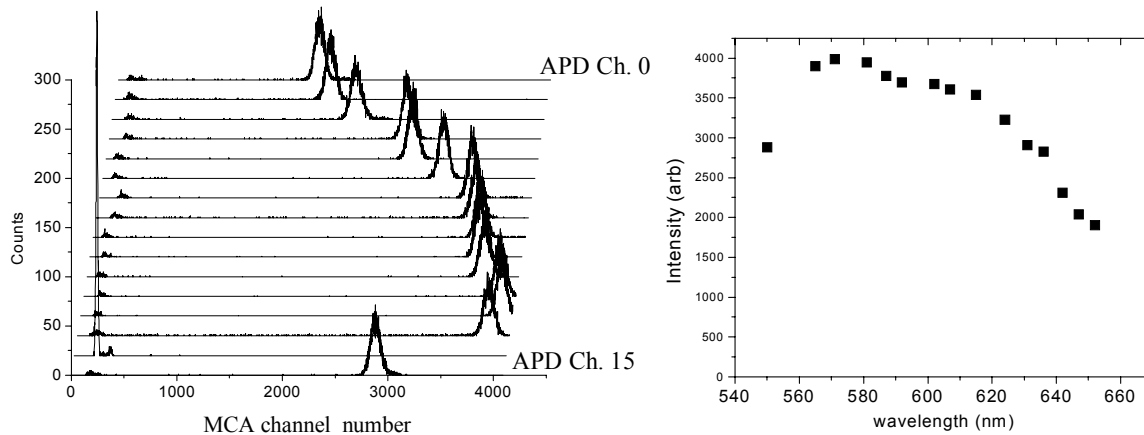


Figure 7: a) Histograms recorded using the APD detector array and the readout ASIC. The source was a white LED with a 2 microsecond pulse width positioned at the iris image plane of the prototype spectrometer. All of the APD channels were recorded simultaneously using the readout ASIC. The ASIC was triggered from the LED signal reflected from the 540 nm beamsplitter to the side scatter PMT. b) The emission spectrum of the white LED derived from the histogram data. The intensity data is not corrected for APD response or gain variations in the array.

## 5. CONCLUSIONS

In this report we have demonstrated the sensitivity and dynamic range of the single element APD detector operating in the visible wavelength region using the six-peak bead set. The emission intensity from these beads is similar to the emission levels expected for working flow cytometer systems, and the performance is comparable to PMT based instruments. The responsivity of the APD is better than the PMT in the near infrared. We report initial studies on cell proliferation measurements that demonstrate application of the APD detector in the near infrared. These results show the improved spectral operating range of the APD detector.

We show that multiple APD elements can be coupled together to create arrays that can detect multiple emission signals from the flow cytometer sample. A prototype instrument is presented that uses a dispersive grating for the separation of the emission wavelengths, and a 16 element APD array for detection of the emission. The instrument uses a proprietary ASIC to simultaneously record the signal intensity measured at each APD channel. With minor modifications this instrument can be used to record 16 fluorescence channels across the visible and near IR spectral regions.

## ACKNOWLEDGEMENTS

The authors would like to gratefully thank Brian Gray and PTI Research, Malvern, PA for providing the CellVue NIR cell tracking dye used in these experiments. The Flow Cytometry Laboratory at Roswell Park Cancer Institute was established in part by equipment grants from the NIH Shared Instrument Program, and receives support from the Core Grant (5 P30 CA016056-29) from the National Cancer Institute to the Roswell Park Cancer Institute. RMD would like to thank NIH for their partial support of this work under grant 1R43CA101266-01.

## REFERENCES

- [1] D. L. Andreas O.H. Gerstner, Wiebke Laffers, Robert A. Hoffman, Michael Steinbrecher, Friedrich Bootz, Attila Tarnok, "Near-Infrared Dyes for Six-Color Immunophenotyping by Laser Scanning Cytometry," *Cytometry*, vol. 48, pp. 115-123, 2002.
- [2] Mitchel L. Woodring, Carleton C. Stewart, E. Podniesinski, and B. Gray, "Flow Cytometry in the Infrared: Inexpensive Modifications to a Commercial Instrument," *Cytometry Part A*, vol. 67A, pp. 104-111, 2005.
- [3] S. N. X. Gao, "Quantum Dot encoded mesoporous beads with high brightness and uniformity: rapid readout using flow cytometry," *Anal. Chem.*, vol. 76(8), pp. 2406-2410, 2004.
- [4] H. O. Z. Zhelev, R. Bakalova, R. Jose, S. Fukuoka, T. Hagase, M. Ishikawa, Y. Baba, "Fabrication of quantum dot - lectin conjugates as novel fluorescent probes for microscopic and flow cytometric identification of leukemia cells from normal lymphocytes," *Chem. Commun.*, vol. 15, pp. 1980-1982, 2005.
- [5] H. R. H. W.A. Bonner, R.G. Sweet, L.A. Herzenberg, "Fluorescence Activated Cell Sorting," *Rev. Sci. Instrum.*, vol. 43, pp. 404-409, 1972.
- [6] P. K. C. Stephen P. Perfetto, and Mario Roederer, "Seventeen-colour flow cytometry: unravelling the immune system," *Nature*, vol. 4, pp. 648-655, 2004.
- [7] R. Farrell, Olschner, F., Frederick, E., McConchie, L., Vanderpuye, K., Squillante, M. R., Entine, G., "Large Area Silicon Avalanche Photodiodes for Scintillation Detectors," *Nucl. Inst. Meth.*, vol. A288, pp. 137, 1990.
- [8] R. Farrell, Redus, R., Gordon, J. S., Gothoskar, P., "High Gain APD Array for Photon Detection," *Proceedings SPIE*, vol. 2550, pp. 266, 1995.
- [9] R. a. B. Poon, C. B., "Cell Tracking Using PKH," in *In living color: protocols in flow cytometry and cell sorting*, S. D. a. R. A. Diamond, Ed. New York: Springer-Verlag, 2000, pp. 302-352.
- [10] N. Bercovici, Givan, A. L., Waugh, M. G., Fisher, J. L., Vernel-Pauillac, F., Ernstoff, M. S., Abastado, J. P., and Wallace, P. K., "Multiparameter precursor analysis of T-cell responses to antigen," *J Immunol Methods*, vol. 276, pp. 5-17, 2003.
- [11] P. K. Wallace, Palmer, L. D., Yang, J. C., Horan, P. K., and Muirhead, K. A., "Mechanisms of adoptive immunotherapy: improved methods for in vivo tracking of tumor infiltrating lymphocytes and lymphokine activated killer cells," *Cancer Research*, vol. 53, pp. 2358-2367, 1993.